

Thermal conductivity and electrical resistivity of the Y- and Er-substituted 1:2:3 superconducting compounds in the vicinity of the transition temperature

B. M. Suleiman, I. Ul-Haq,* E. Karawacki, A. Maqsood,* and S. E. Gustafsson
Department of Physics, Chalmers University of Technology, S-412 96 Gothenburg, Sweden

(Received 13 July 1992; revised manuscript received 8 March 1993)

The thermal conductivity and electrical resistivity of $\text{ErBa}_2\text{Cu}_3\text{O}_{7-\delta}$ and $\text{YBa}_2\text{Cu}_3\text{O}_{7-\delta}$ sintered compounds have been measured to investigate the electron-phonon interaction in the vicinity of T_c in these materials. The thermal conductivity was measured using the transient-plane-source technique. With the electrical-resistivity data and Wiedeman-Franz law, the magnitude of the free-carrier component of the thermal conductivity has been estimated to less than 15% of the measured thermal conductivity. The results in the normal state are interpreted in terms of two models. The first model is the ordinary electron-phonon transport theory applied to high- T_c superconductors, and the second model is the Bardeen-Rickayzen-Tewordt (BRT) theory of the lattice heat conduction in high- T_c superconductors. Both models suggest that the electron-phonon coupling varies from moderately weak to strong coupling depending on characteristic parameters of the considered material such as oxygen content, porosity, T_c value, ΔT_c , etc., all of which are directly related to the purity of the investigated samples. Furthermore, using this transient technique a dramatic increase of the thermal conductivity is observed below T_c and the experimental results are in reasonable agreement with the prediction of the generalized BRT theory, adapting a weak coupling with scaled-BCS-gap formalism for the moderately-weak-coupling sample and a strong coupling s -wave-pairing formalism for the strong-coupling sample.

INTRODUCTION

The interpretation of the thermal and other transport properties of high-temperature superconductors is intricate, since even assuming a conventional boson-exchange mechanism for the superconductivity one cannot use the simple BCS formalism. The reason may be due to the fact that the data are consistent with a moderate to strong coupling.

Two different approaches were used previously to estimate the carrier-phonon coupling constant λ from the electrical resistivity and thermal conductivity data in the normal state. The first one is the ordinary electron-phonon transport theory applied to high- T_c superconductors, and the second one is the Bardeen-Rickayzen-Tewordt (BRT) theory of the lattice heat conduction. The results are, however, rather inconsistent, in some cases when using BRT theory under the same assumptions (weak-coupling and s -wave pairing states) one obtains weak coupling but with an order of magnitude difference in the coupling strength between crystals and sintered samples. On the other hand the application of the electron-phonon transport theory on a sintered sample leads to quite a strong coupling with a λ value much higher than 1. One possible explanation of this diversity may be due to experimental inconsistency such as poor definition of the investigated samples or the experimental technique used.

Although most of the reported data from thermal conductivity measurements of the high-temperature superconducting materials—polycrystalline¹⁻³ or single crystal⁴⁻⁷—exhibit a common behavior of increase of the thermal conductivity below T_c , the agreement be-

tween the absolute values of the thermal conductivity for similar compounds is rather moderate. This may be due to poor definition of the investigated samples in terms of common characterization parameters such as the oxygen content and the degree of porosity for polycrystalline samples. These factors are likely to affect the magnitude as well as the temperature dependence of the thermal conductivity of these materials. Polycrystalline (sintered) samples should preferably be carefully characterized as far as the above-mentioned two factors are concerned. It seems that this is the only way to reach agreement on how to describe the behavior of the investigated materials. The new information from studying sintered samples should be related to their thermal behavior, which may lead to different λ values depending on their characteristic parameters, in contrast to the pure crystals where the nature of the coupling is expected to be of the same type.

The ideal experimental situation in case of materials exhibiting variations in porosity and the content of different constituents is to determine the different macroscopic parameters (in this case electrical resistivity and thermal conductivity) for the same sample. If this is not possible, one should preferably use samples made from the same batch, a procedure adopted for the measurements presented in this work. This procedure made it possible for us to properly relate the electrical resistivity and thermal conductivity and then estimate the coupling between electrons and phonons, which appeared to be neither weak nor very strong, but it depends on the characteristic parameters of the sample.

For the study of thermal conductivity the new transient plane source (TPS) method has been introduced and a rapid rise in the thermal conductivity below T_c was ob-

served. While the behavior of the thermal conductivity above T_c follows a familiar pattern, the increase below T_c is very rapid. The commonly used steady-state technique gives an increase of the thermal conductivity in sintered samples of approximately 15% over an interval of about 40 K below T_c . Our results, however, show a much more rapid rise of the thermal conductivity, which may be attributed to a larger phonon contribution in the heat conduction below T_c for this type of samples.

In our measurements care was taken not to increase the temperature in the sample more than 0.1 K (which corresponds to an average temperature gradient of 0.02 K/mm) with a view to map any temperature dependence if the measurements would indicate a rapidly varying thermal conductivity. With temperature differences across the sample of the order of degrees one would definitely smear out the temperature dependence by referring to the actual measured values. If an experimental method does require temperature difference of the order of degrees, which is not uncommon for the steady-state methods, it is important to remember that the experimental values should be viewed as mean values over the temperature difference used in the actual recordings. Moreover, according to Uher⁸ the accuracy of the longitudinal steady-state technique, so far used for determination of the thermal conductivity of the superconducting compounds, seems to be affected by radiative heat losses down to 200 K.

An advantage of the TPS method is that the thermal radiation into the surroundings from the sample boundaries are eliminated, since the transient recording is terminated before the thermal wave reaches the boundaries. The only influence from thermal radiation in these experiments is coupled to possible radiative processes inside the sample material. This radiation process is present also when using the steady-state technique.

A further advantage of the rather small temperature increases in the relatively large samples is the possibility of substantially reducing the convective heat mechanism.^{9,10} It has been suggested that this mechanism is related to the temperature gradient across the sample, and it has been proposed that this should be adopted as an explanation of the increase of thermal conductivity below T_c .

EXPERIMENT

The thermal conductivity k of $\text{YBa}_2\text{Cu}_3\text{O}_{7-\delta}$ and $\text{ErBa}_2\text{Cu}_3\text{O}_{7-\delta}$ superconducting compounds was measured between 77 and 295 K using the recently developed transient plane source (TPS) technique.¹¹ The technique

is an extension of the known transient hot strip^{12,13} (THS) method. The experimental arrangements for the TPS method are rather simple. A disk-shaped TPS element with the approximate dimensions 0.07-mm thickness and an effective diameter of 20 mm is placed between two cylindrical pieces of the sample material. In the present work each piece had a diameter of 28 mm and a thickness of 10 mm. The size of samples used for the thermal conductivity measurements was in fact the largest reported for this kind of measurements.

When measuring the thermal transport properties at a particular temperature, the sample is left in the cryostat until all temperature gradients have disappeared. After having achieved isothermal conditions in the sample, a constant current pulse is passed through the element while simultaneously recording the voltage (resistance/temperature) increase in the element. The TPS element is used both as heat source and temperature detector.

The technique is based on a three-dimensional heat flow inside the sample, which can be regarded as an infinite medium by limiting the total time of the transient recording. The different pieces of apparatus involved in these measurements are given elsewhere.¹⁴ In addition to the thermal conductivity, it is also possible to extract information on the thermal diffusivity from the measured data although with a slightly lower accuracy.

The measurements of the electrical resistance were performed by the standard dc four-point method with a measuring current of 20 mA corresponding to a current density of 0.45 A/cm², and the samples for these measurements were made from the same batch and cut from smaller pellets (13-mm-diam) in the form of parallelepipeds with dimensions given in Table I.

The samples were prepared using the solid-state sintering technique. Y_2O_3 , Er_2O_3 , CuO, and BaCO_3 , 99.99% pure oxides, were mixed and ground in an agate mortar. The mixture was calcined as loose powder at 900 °C in air for 20 h and then cooled to room temperature in air. The black powder was reground and sintered again in 920 °C for 20 h and then cooled to room temperature in air. Again the powder was reground and pressed into pellets, sintered for 20–24 h at 940 ± 5 °C, and the sample was left to cool in air till the furnace reached room temperature. Finally the furnace was heated up to 400 ± 5 °C and kept at this temperature for another 48 h in oxygen atmosphere, and the whole arrangement was left to cool down to room temperature.

The oxygen content was determined by the wet chemical method, and the results are $\delta=0.01$ for the Y-based sample and $\delta=0.12$ for the Er-based sample. The x-ray

TABLE I. The characterizing parameters for both samples. D_m and D_c are the corresponding measured and calculated densities, r is the porosity, A is representing the defect and impurities resistivity, and α is the temperature coefficient of resistivity (for more details see text).

Sample	D_m (g cm ⁻³)	D_c (g cm ⁻³)	r	Dimensions (mm ³)	T_0 (K)	ΔT_c (K)	T_c (K)	A (mΩ cm)	α (μΩ cm K ⁻¹)
$\text{YBa}_2\text{Cu}_3\text{O}_{6.99}$	5.08	6.36	0.20	4.40 × 4.3 × 1.0	85	1.2	91.5	0.049	4.42
$\text{ErBa}_2\text{Cu}_3\text{O}_{6.88}$	5.4	7.13	0.24	4.86 × 4.3 × 1.0	82	4	87	1.43	3.97

analysis showed a single-phase orthorhombic structure with the following unit-cell dimensions: $a = 3.821 \text{ \AA}$, $b = 3.887 \text{ \AA}$, $c = 11.68 \text{ \AA}$ for the Y-based sample and $a = 3.890 \text{ \AA}$, $b = 3.817 \text{ \AA}$, $c = 11.648 \text{ \AA}$ for the Er-based sample.

RESULTS

The resistivity measurements are shown in Fig. 1. Both samples show a sharp superconducting transition. The width of the transition ΔT_c (defined as the 10–90 % transition), the midpoint of the transition T_c and the zero resistance temperature T_0 are all given in Table I. The electrical resistivity at higher temperature in the normal state for both samples increases linearly with temperature. The onset temperature of the linear behavior is around 100 K. A slight deviation from linearity is observed around 210 K for the Y-based sample, which is particularly interesting, since a similar deviation has been reported elsewhere.²

The thermal conductivity data in the vicinity of T_c are shown in Fig. 2. At T_c there is a net change in the slope of the curve for both samples, with a very dramatic increase near T_c . This observation, as far as the size of the increase is concerned, is in contrast to a series of earlier measurements, where only an increase of approximately 10–20 % has been reported (see Discussion). Moreover, to assure the validity of this increase we have evaluated the data by using extreme constrains in the computational procedure and the result is that the scattering from the mean values is less than 5%, except for specific points where the possible deviation from the mean is indicated by the bars in the figures. Figure 2(a) indicates that the thermal conductivity for the Y-based sample increases with increasing temperature above T_c and then decreases slowly up to room temperature. Figure 2(b) shows a slight steady increase of the thermal conductivity for the Er-based sample for $T > T_c$ up to room temperature. The Y-based sample has reasonably higher values of k as is expected from the porosity values, however the upturn of k just below T_c is less sharper than for the Er-based sample.

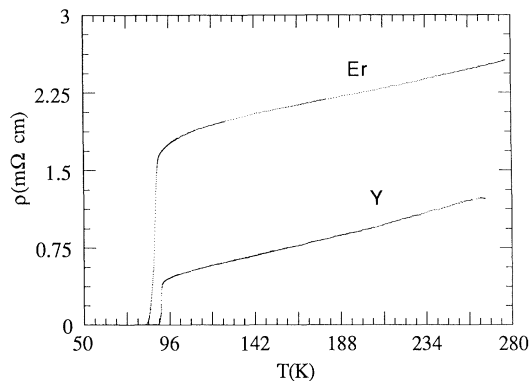


FIG. 1. The temperature dependence of the electrical resistivity of both samples. At higher temperature the electrical resistivity increase linearly with temperature having a higher slope for the Y-based sample.

Since the electrical resistivity above T_c is relatively large and varies linearly with temperature, which suggests that the scattering of the charge carriers can be mainly by phonons in this temperature range, Matthiessen's rule may be used to fit the resistivity data to a straight line. The slope of this line α will give an estimation of the resistivity change due to scattering by phonons. At the same time, the intercept A is an estimation of the scattering by impurities and defects. The values of α and A are given in Table I.

The samples have been prepared by grinding, pressing, and sintering processes, which involve nondetermined stresses and creation of voids. Thus a characterizing parameter such as porosity should be defined for the investigated samples. An estimation of the porosity can be determined using the following formula:

$$r = 1 - (D_m / D_c) \quad (1)$$

where D_m is the measured apparent density of the sample and D_c is the calculated density based on the atomic weights of the constituting atoms and the dimensions of

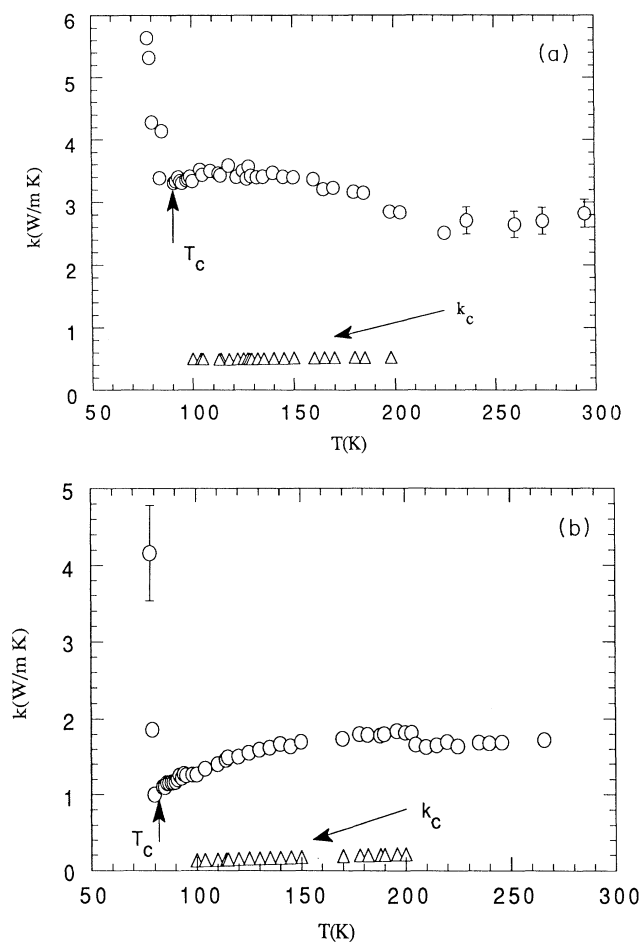


FIG. 2. The thermal conductivity data of (a) $\text{YBa}_2\text{Cu}_3\text{O}_{6.99}$ and (b) $\text{ErBa}_2\text{Cu}_3\text{O}_{6.88}$ against temperature, (Δ) represent the carrier contribution to k as indicated by the inclined arrows, the vertical arrows indicate the corresponding T_c 's.

the unit cell. The r values are also given in Table I. It should be noted that the Er-based sample is more porous than the other sample, and therefore it has more voids or less conduction channels for the carriers, which leads to a higher resistivity. Higher porosity also influences the thermal conduction by phonons, since voids serve as scattering centers for phonons and take up a fraction of the heat conduction volume of the material leading to a lower thermal conductivity.

DISCUSSION

To interpret the thermal conductivity behavior in the vicinity of T_c in connection with the linearity in the electrical resistivity behavior of the high- T_c oxides in general, one may assume the validity of Mathiessen's rule and express the relative contributions of the carriers conduction k_c and lattice conduction k_L to the total thermal conductivity as

$$k = k_c + k_L . \quad (2)$$

Assuming an elastic scattering, an upper limit to the carriers thermal conductivity in the normal state can be calculated using the Wiedemann-Franz law.

$$k_c = L_0 T \rho^{-1} , \quad (3)$$

where $L_0 = 2.45 \times 10^{-8} \text{ V}^2 \text{ K}^{-2}$.

An estimation of k_c is also shown in Fig. 2. It should be noted that the estimated k_c values do not exceed 15% of the total thermal conductivity in the relevant temperature range. Thus the largest contribution to the total thermal conductivity above T_c seems to be due to lattice conduction.

The sharp upturn of the measured thermal conductivity and the further increase for $T < T_c$ may arise from the decrease in scattering of phonons by carriers as they condense into superconducting pairs. This would cause a faster increase of k_L , which predominates the decrease in k_c leading to a net increase in the measured thermal conductivity.

Even though our observation of the rapid rise of the thermal conductivity [amounting to $k(78 \text{ K})/k(200 \text{ K}) \approx 1.8$ for the Y-based sample and $k(78 \text{ K})/k(200 \text{ K}) \approx 2$ for the Er-based sample] has been verified via the specific heat (C) values, which may be estimated from the formula $CD_m = k/\kappa$, where κ is the thermal diffusivity, it still might not be possible from these measurements to give a definite physical meaning to this rapid increase. It is worth mentioning at this point that a rapid increase in k has been reported recently by Yu *et al.*¹⁵ for untwinned $\text{YBa}_2\text{Cu}_3\text{O}_{7-\delta}$ single crystal, which has a rise at the peak amounting to $k_a(50 \text{ K})/k_a(200 \text{ K}) \approx 2.8$, and they attribute this effect in the superconducting state to the electronic contribution of the Cu-O plane. It should be noted that the viewpoint adopted in Ref. 15 is unlike the common scenario that attributes the thermal conductivity enhancement in the superconducting state to the phononic contribution. The role of phononic contribution in the enhancement of k below T_c is formally predicted by the BRT theory for high- T_c superconductors and also

justified by thermal conductivity measurements of $\text{YBa}_2\text{Cu}_3\text{O}_{7-\delta}$ single crystals in a magnetic field.¹⁶ Likewise, the analysis of our data turns out to be in the favor of this common scenario because it leads to a good agreement with the predication of BRT theory.

In order to estimate the phonon-electron interaction strength of the above compounds, we have used two approaches: The first one is applying the model usually used for metals in the vicinity of T_c , where the phonon-phonon scattering is relatively small. This approach and similar analysis was previously done by Heremans *et al.*,³ and, in principle, we are following their heuristic arguments. The second approach is the Bardeen-Rickayzen-Tewordt^{17,18} (BRT) theory of the lattice conduction in high- T_c superconductors, up to 180 K.

Based on the linear behavior of the electrical resistivity and the relatively weak temperature dependence of k_L in the normal state, we have used the first approach in the vicinity of T_c at 100 K, where the onset of the linear resistivity behavior begins. Where it may be assumed that the phonons are mainly scattered by carriers, following the procedure of Heremans *et al.*³ we estimate the value of electron-phonon interaction strength by exploiting the model usually applied to metals.

We may start by estimating the number of electrons per unit cell n_a in the normal state from the relation between the lattice thermal conductivity and the electrical resistivity¹⁹

$$k_L \rho / T \geq (k_B / e)^2 (C / C_{\max})^2 (1 / n_a^2) , \quad (4)$$

where e is the electron charge, k_B is Boltzmann constant and $C_{\max} = 3Nk_B$ is the theoretical Dulong-Petit value of the specific heat C . From the density, the atomic weights of each compound and n_a the electron density n for each sample can be deduced.

The phonon limited electrical resistivity ρ_{c-p} can be expressed as

$$1 / \rho_{c-p} = en\mu , \quad (5)$$

where μ is the carriers mobility. Then from μ the carrier-phonon scattering relaxation time τ_{c-p} can be calculated by considering the effective mass m^* to be equal to the free-electron mass and using the relation $\mu = e\tau_{c-p}/m^*$. The above calculated parameters at 100 K are given in Table II. The obtained values for n and τ_{c-p} still suggest that we may consider the behavior of the carriers as free carriers and not localized ones.

In spite of the fact that the primary argument in this approach is not based on Boltzmann equation, but in order to estimate the magnitude of carrier-phonon coupling constant λ_{c-p} , we further use the lowest-order variational solution of Bloch-Boltzmann equation from which λ_{c-p} is calculated²⁰

$$\hbar / \tau_{c-p} = 2\pi\lambda_{c-p}k_B T . \quad (6)$$

The values of λ_{c-p} in Table II for the $\text{ErBa}_2\text{Cu}_3\text{O}_{7-\delta}$ indicate a strong coupling ($\lambda_{c-p} > 1$), while the corresponding value for $\text{YBa}_2\text{Cu}_3\text{O}_{7-\delta}$ falls little below that range. These values were quite different from the values previ-

TABLE II. The calculated parameters at 100 K. k_c and k_L are the corresponding carriers and lattice thermal conductivities, n_d is the number of electrons per unit cell, n is the carriers densities, τ_{c-p} is the relaxation time, and λ_{c-p} is the carrier-phonon coupling constant, details are given in the text.

Sample	k_c (W m ⁻¹ K ⁻¹)	k_L (W m ⁻¹ K ⁻¹)	$\frac{C}{C_{max}}$	n_d	n (10 ²¹ cm ⁻³)	τ_{c-p} (10 ⁻¹⁴ sec)	λ_{c-p}
YBa ₂ Cu ₃ O _{6.99}	0.50	2.84	0.43	0.29	1.3	1.27	0.95
ErBa ₂ Cu ₃ O _{6.88}	0.14	1.14	0.81	0.24	1.0	0.43	2.7

ously reported,³ which were $\lambda_{c-p}=6$ for similar samples, i.e., far into the strong-coupling range.

Following Tewordt and Wölkhausen,^{17,18} Peacor *et al.*⁷ and Cohn *et al.*,⁵ the lattice thermal conductivity is not limited only by the scattering of carriers but also by the phonon-phonon and defect-phonon scattering. An estimation of the relative magnitude of these scattering mechanisms may be obtained from a calculation using the BRT theory within a certain temperature range above T_c .

Using the BRT theory within the Debye framework and neglecting the polarization, the lattice contribution^{7,5} of thermal conductivity for the sintered samples may be expressed as

$$k_L(T) = \frac{k_B}{2\pi^2v} \left[\frac{k_B T}{\hbar^3} \right]^3 \int_0^{\Theta_D/T} dx \frac{x^4 e^x}{(e^x - 1)^2} \tau(T, x). \quad (7)$$

Here x is the reduced phonon energy $x = \hbar\omega/k_B T$, $v = 5000$ m sec⁻¹ is the sound velocity,^{17,5} Θ_D is the Debye temperature and

$$\tau^{-1}(T, x) = S_b + S_d(xT)^4 + S_e x T g(x, T) + S_p x^2 T^4, \quad (8)$$

where $g(x, T)$ is the ratio of the phonon-carrier scattering rates in the normal and the superconducting states. In the BRT theory, $g(x, T)$ is proportional to the ratio of the phonon-electron scattering times in the normal and superconducting states τ_{pe}^n/τ_{pe}^s , this being equal to unity in the normal state and being a universal function of $\Delta/(k_B T)$ in the superconducting state, where Δ is the superconducting gap.

The coefficients S_b , S_d , and S_e , and S_p describe the magnitude of the phonon scattering by boundaries, point defects, carriers, and other phonons, respectively. We have limited the fitting parameters for the phonon-defects scattering rates only to point defect scattering rate S_d by ignoring the small contribution from the scattering of phonons by the strain fields of sheetlike faults and dislocations following the same argument as given by Ref. 5.

Examining Eq. (7) more carefully, we can see that for the normal state the phonon-defect and phonon-carriers scattering contributions are weakly temperature dependent. Furthermore the relative importance of a particular scattering mechanism with respect to the other mechanisms can be determined by switching off that particular mechanism and then evaluating the integral (see Fig. 3 in Ref. 7).

Table III shows the estimated coefficients by numerically integrating Eq. (7) and fitting the normal-state data k_L up to 180 K, using $\Theta_D = 400$ K for the Y-based sample²¹ and $\Theta_D = 350$ K for the Er-based sample.²² Seeking a minimum deviation of the experimental data around the theoretical curve, the best fits were obtained when the mean deviation of the experimental data was less than $\pm 0.5\%$ for the Y-based sample and less than $\pm 0.3\%$ for the Er-based sample. This agreement may have a certain degree of randomness either because of the approximations used when applying the theory or the possibility of getting an acceptable fit to the data with more than one combination of the determined coefficients. However, our values of these coefficients may be given physical meaning as we will see later.

The coefficient S_b due to the boundaries scattering is expected to affect the shape of the theoretical curve only at low temperatures, since at these temperatures the microstructure of the sample will determine the boundary-phonon scattering. The coefficient can be expressed as $S_b = v/L$, where L is the crystalline thickness for crystals or it is the average length between the boundaries of a grain for the sintered samples. Based on $5 \mu\text{m}$ as a typical length of the phonon mean free path⁷ at 77 K and on the microstructure analysis of sintered materials,^{21,23} we used a value for $L = 2 \mu\text{m}$ as a typical grain size for the sintered samples. It should be noted that for the normal state, the boundary term in Eq. (8) is less effective than the other terms and could have an order of magnitude variation and still be acceptable without essentially affecting the total scattering rate.

The point defect scattering coefficient S_d for the Y-

TABLE III. Debye temperature Θ_D and a list of the theoretical coefficients given by Eqs. (8), (9), and (10), where S_b , S_d , S_e , and S_p are the phonon-scattering coefficients used to fit Eq. (8), λ is the phonon coupling constant given by Eq. (9), and γ is a coefficient related to S_e in Eq. (10).

Sample	Θ_D (K)	S_b (sec ⁻¹)	S_d (K ⁻⁴ sec ⁻¹)	S_e (K ⁻¹ sec ⁻¹)	S_p (K ⁻⁴ sec ⁻¹)	λ	γ
YBa ₂ Cu ₃ O _{6.99}	400	2.5×10^9	10	3.7×10^9	530	0.94	135
ErBa ₂ Cu ₃ O _{6.88}	350	2.5×10^9	150	8.1×10^9	30	2.1	279

based sample is much less than the corresponding value for the Er-based sample as expected from the porosity and oxygen contents analysis. The phonon-carrier scattering coefficient S_e is likely to have values one or two orders of magnitude higher than the corresponding values reported for single crystals.^{7,5} According to Tewordt and Wölkausen¹⁷ this coefficient is ideally related to the phonon-carriers coupling constant for the longitudinal acoustic phonons,

$$\lambda = \frac{2}{\pi} t \frac{a}{v} S_e, \quad (9)$$

where $t = 5000$ K is the effective hopping matrix element for a two-dimensional tight-binding band of electrons,¹⁷ and $a = 4$ Å is the average lattice constant. The calculated values of λ when using Eq. (9) are given in Table III. These values are in rather good agreement with our values obtained from the first approach given in Table II but they are quite different from the values previously reported,^{7,17} which lay in the weak-coupling range.

Relating λ from Eq. (9) to the γ coefficient in Ref. 17, we get an expression for γ as

$$\gamma = \frac{S_e T_c L}{v}. \quad (10)$$

The values for γ are also shown in Table III. It should be noted that γ for the Y-based sample is smaller than the corresponding value for the Er-based sample, i.e., a higher value of γ implies lower conductivity sample in the normal state, which is in good agreement with Refs. 17 and 18 (see Fig. 2 in Ref. 17 or Fig. 3 in Ref. 18).

The phonon-phonon scattering coefficient S_p is larger for the Y-based sample. A smaller value means that the role of phonon-phonon scattering mechanism is minimized. This may explain the slight increase of the k values of the Er-based sample [Fig. 2(b)] for $T > T_c$, and it is in rather good agreement with analysis of the importance of this mechanism as shown in Fig. 3 of Ref. 7. Since the variations in the theoretical coefficients for the two samples correspond to the quantitative differences in the microstructure, which are related to characteristic parameters of the materials such as porosity, oxygen content, etc., our analysis may provide further evidence for successfully applying Eq. (7) for sintered samples.

Regarding earlier analysis^{5,7,17} including ours, it may be noted that the absolute values of the theoretical coefficients defined by Eq. (8) are varying from sample to sample depending on the sample type (e.g., comparing crystal to crystal, sintered sample to sintered sample, or crystal to sintered sample). It seems as if the relative magnitude of these coefficients for the same sample is more significant than their absolute values from different samples.

In order to relate some physical meaning to the rapid rise in k just below T_c when applying the BRT theory, we need to know the electronic contribution in the heat conduction below T_c , and in fact it is not a simple task to estimate k_c . Previously, Peacor *et al.*⁷ estimated k_c by using a tabulated ratio of the electronic thermal conductivity in the superconducting and normal states for $T < T_c$,

and Cohn *et al.*⁵ made no assumptions regarding the behavior of k_c at $T \leq T_c$, but they used upper and lower limits for k_c by employing the temperature dependent Lorenz number L_e usually applied for pure metals.

However, the few data points we have below T_c for k suggest to us that the role of k_c in the heat conduction in the vicinity of T_c is relatively small and the major role in these kind of samples is mainly due to the phonon contribution. This may be justified by examining the analysis done by Tewordt and Wölkausen,¹⁸ more specifically looking at the calculated isotropic phonon thermal conductivity k_g depicted in Fig. 2 in Ref. 18, where they utilized the same fitting parameters previously¹⁷ used to fit the data of sintered samples. The sharp rise of the k_g [estimated $k_g(78 \text{ K})/k_g(1.5T_c) \approx 2.0$], which was calculated based on strong coupling for s -wave pairing [using $\lambda = 2.3$ that yielded $T_c \approx 90$ K and $\Delta/(K_B T) \approx 6$] is in a good agreement with sharp rise of our Er-based sample ($\lambda = 2.1$). On the other hand our data for the Y-based sample ($\lambda = 0.94$) indicate that the sharp rise is in agreement with the rise of the weak-coupling isotropic phonon thermal conductivity [estimated $k_g(78 \text{ K})/k_g(1.5T_c) \approx 1.6$], which was calculated by scaling the BCS gap $\{\Delta(0)/\Delta_{\text{BCS}}(0) = 1.7\}$ and we believe that a larger scaling will yield better agreement, see also Fig. 2 Ref. 17.

In conclusion our analysis using both models suggests firstly that the two models are in a reasonable agreement concerning the spread of the λ value between the two samples and secondly that the characteristic parameters such as the porosity, oxygen content, T_c value and ΔT_c are factors contributing to the nature of the phonon-carrier interaction and that their values are essential to determine the nature of coupling. Obviously the above consideration should only be taken as an indication of the presence of both strong and moderately weak electron-phonon coupling in these types of high-temperature superconductors. It should be noted that there is a degree of uncertainty in determining the λ values due to the fact that there are many approximations involved in using these two models. Some of these approximations are introduced when using the first model, where we have exploited the formulas usually applied to metals, or when using the BRT theory by referring only to the role of the longitudinal-acoustic phonons in the lattice heat conduction. However, of these two models it is more logical to rely on the λ values obtained by applying the BRT theory.

Returning to the importance of using the transient techniques, we would like to refer to the ability of these techniques in probing the dynamic behavior of this kind of materials. Looking at the experimental observations, with the temperature dependence of the thermal conductivity depicted in Figs. 2(a), 2(b), and 3, we note a very dramatic increase near T_c .

As it was pointed out in the Discussion, we are not able to give a definite explanation to the observation of this dramatic increase of the thermal conductivity and to the fact that this rapid increase has not been observed before. However, it should be noted that we have used a quite

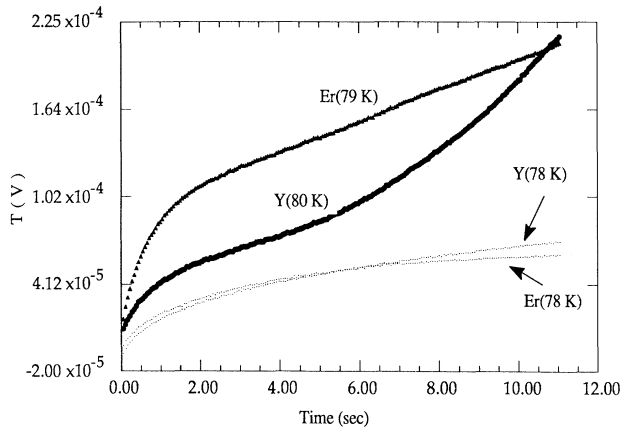


FIG. 3. The voltage recording at different temperatures for the superconducting samples, the lower two curves at 78 K are representing the standard recording, while the higher ones are showing the dramatic variations in the thermal conductivity at 80 K for the Y-based sample and at 79 K for the Er-based sample.

different experimental technique for measuring the thermal properties.

In earlier measurements the steady-state method has been used exclusively, while in this work we have used a transient technique. There are a few important differences between these methods, that should be noted, when making an assessment of the experimental observations.

(a) The steady-state method, as used in the earlier measurements, has been applied with a rather large temperature difference—of the order of degrees—which implies a higher temperature gradient within the sample.

(b) The geometrical arrangement (length and cross section of the sample) of the steady-state method is quite different for a material with high thermal conductivity, as compared with a material with low thermal conductivity.

(c) The new TPS method has been applied in a large number of measurements on materials with thermal con-

ductivity within a range from 0.02 up to 200 W/m K—using similar sample dimensions and the same TPS elements as in the present work and the results are in good agreement with existing data.

(d) The temperature difference utilized in the transient (TPS) recordings have all been kept below 0.1 K in order to avoid any “smearing out” effect that might occur if a large temperature difference would be imposed on the sample.

(e) The results depicted in Fig. 3 indicate that the properties are changing very dramatically close to T_c . The curves marked Y (78 K) and Er (78 K) are standard recordings of the temperature (or voltage) versus time, from which the thermal conductivity is being routinely calculated. However, when going to the curves marked Er (79 K) and Y (80 K) only one or two degrees higher, we get indications of the dramatic variations in the thermal conductivity. We can actually see that the sample changes properties during the transient recording in spite of the very small temperature increase of the TPS element. Looking at curve Y (80 K) only the very first part of the transient (perhaps up to 2 sec) can be utilized for evaluating the properties. The reason is that the sample seems to retain “constant” properties only for very small temperature increases.

Further work is being planned with a view to look in this particular temperature range perhaps also using somewhat different experimental techniques such as the dynamic plane source^{24,25} (DPS) technique.

ACKNOWLEDGMENTS

We thank P. Berastegui from the Department of Inorganic Chemistry at Chalmers University of Technology for the assistance with the determination of the oxygen content. The work has been financially supported by the Swedish Natural Science Research Council, Anna Ahrenbergs fond för vetenskapliga ändamål, and the National Swedish Board for Technical Development. Two of us (I.U.) and (A.M.) acknowledge with thanks support from ISP in Uppsala, Sweden.

*Present address: Department of Physics, Quaid-i-Azam University, Islamabad, Pakistan.

¹V. Bayot, F. Delannay, C. Dewitte, J.-P. Erauw, X. Gonze, J.-P. Issi, A. Jonas, M. Kinany-Alaousi, M. Lambrecht, J.-P. Michenaud, J.-P. Minet, and L. Piraux, *Solid State Commun.* **63**, 983 (1987).

²A. Jezowski, J. Mucha, K. Rogacki, R. Horyn, Z. Bukowski, M. Horobowski, J. Rafalowicz, J. Stepien-Damm, C. Sulkowski, E. Trosnar, A. J. Zaleski, and J. Klamut, *Phys. Lett. A* **122**, 431 (1987).

³J. Heremans, D. T. Morelli, G. W. Smith, and S. C. Strite III, *Phys. Rev. B* **37**, 1604 (1988).

⁴J. L. Cohn, S. A. Wolf, and T. A. Vanderah, *Phys. Rev. B* **45**, 511 (1992).

⁵J. L. Cohn, S. A. Wolf, T. A. Vanderah, V. Selvamnickam, and K. Salama, *Physica C* **192**, 435 (1992).

⁶S. J. Hagen, Z. Z. Wang, and N. P. Ong, *Phys. Rev. B* **40**, 9383 (1989).

⁷S. D. Peacor, R. A. Richardson, F. Nori, and C. Uher, *Phys. Rev. B* **44**, 9508 (1991).

⁸C. Uher, *J. Supercond.* **3**, 337 (1990).

⁹C. Gorter, *Can. J. Phys.* **34**, 1334 (1956).

¹⁰V. L. Gunzburg, *J. Supercond.* **2**, 323 (1989).

¹¹S. E. Gustafsson, *Rev. Sci. Instrum.* **62**, 797 (1991).

¹²S. E. Gustafsson, E. Karawacki, and M. N. Khan, *J. Phys. D* **52**, 259 (1981).

¹³S. E. Gustafsson, E. Karawacki, and M. A. Chohan, *J. Phys. D* **19**, 727 (1986).

¹⁴B. M. Suleiman, I. Ul-Haq, E. Karawacki, and S. E. Gustafsson, *J. Phys. D* **25**, 813 (1992).

¹⁵R. C. Yu, M. B. Salamon, Jian Ping Lu, and W. C. Lee, *Phys. Rev. Lett.* **69**, 1431 (1992).

- ¹⁶R. A. Richardson, S. D. Peacor, Franco Nori, and C. Uher, *Phys. Rev. Lett.* **67**, 3856 (1991).
- ¹⁷L. Tewordt and Th. Wölkhausen, *Solid State Commun.* **70**, 839 (1989).
- ¹⁸L. Tewordt and Th. Wölkhausen, *Solid State Commun.* **75**, 515 (1990).
- ¹⁹J. M. Ziman, *Electrons and Phonons* (Clarendon, Oxford, 1960).
- ²⁰P. B. Allen, T. P. Beaulac, F. S. Khan, W. H. Butler, F. J. Pinski, and J. C. Swihart, *Phys. Rev. B* **34**, 4331 (1986).
- ²¹A. Junod, *Physical Properties of High Temperature Superconductors*, edited by D. M. Ginsberg (World Scientific, Teaneck, NJ, 1990), Vol. 2.
- ²²H. D. Yang, H. C. Ku, P. Klavin, and R. N. Shelton, *Phys. Rev. B* **36**, 8791 (1987).
- ²³R. S. Nakahara, G. J. Fisanick, M. F. Yan, R. B. van Dover, and T. Boone, *Appl. Phys. Lett.* **53**, 2105 (1988).
- ²⁴E. Karawacki and B. M. Suleiman, *Meas. Sci. Technol.* **2**, 744 (1991).
- ²⁵E. Karawacki, B. M. Suleiman, I. Ul-Haq, and Bui-Thi-Nhi, *Rev. Sci. Instrum.* **63**, 4390 (1992).